Bile-acid-mediated decrease in endoplasmic reticulum stress: a potential contributor to the metabolic benefits of ileal interposition surgery in UCD-T2DM rats

Bethany P. Cummings[1,2,*], Ahmed Bettaieb[2], James L. Graham[1,2], Jaehyoung Kim[3], Fangrui Ma[3], Noreene Shibata[2], Kimber L. Stanhope[1,2], Cecilia Giulivi[1,4], Frederik Hansen[5], Jacob Jelsing[5], Niels Vrang[5], Mark Kowala[6], Michael L. Chouinard[6], Fawaz G. Haj[2] and Peter J. Havel[1,2]

SUMMARY

Post-operative increases in circulating bile acids have been suggested to contribute to the metabolic benefits of bariatric surgery; however, their mechanistic contributions remain undefined. We have previously reported that ileal interposition (IT) surgery delays the onset of type 2 diabetes in UCD-T2DM rats and increases circulating bile acids, independently of effects on energy intake or body weight. Therefore, we investigated potential mechanisms by which post-operative increases in circulating bile acids improve glucose homeostasis after IT surgery. IT, sham or no surgery was performed on 2-month-old weight-matched male UCD-T2DM rats. Animals underwent an oral fat tolerance test (OFTT) and serial oral glucose tolerance tests (OGTT). Tissues were collected at 1.5 and 4.5 months after surgery. Cell culture models were used to investigate interactions between bile acids and ER stress. IT-operated animals exhibited marked improvements in glucose and lipid metabolism, with concurrent increases in postprandial glucagon-like peptide-1 (GLP-1) secretion during the OFTT and OGTTs, independently of food intake and body weight. Measurement of circulating bile acid profiles revealed increases in circulating total bile acids in IT-operated animals, with a preferential increase in circulating cholic acid concentrations. Gut microbial populations were assessed as potential contributors to the increases in circulating bile acid concentrations, which revealed proportional increases in *Gammaproteobacteria* in IT-operated animals. Furthermore, IT surgery decreased all three sub-arms of ER stress signaling in liver, adipose and pancreas tissues. Amelioration of ER stress coincided with improved insulin signaling and preservation of β-cell mass in IT-operated animals. Incubation of hepatocyte, adipocyte and β-cell lines with cholic acid decreased ER stress. These results suggest that post-operative increases in circulating cholic acid concentration contribute to improvements in glucose homeostasis after IT surgery by ameliorating ER stress.

INTRODUCTION

Bariatric surgery, such as Roux-en-Y gastric bypass (RYGB), is currently the most effective treatment for obesity and often results in type 2 diabetes resolution and possibly type 2 diabetes prevention (Buchwald et al., 2004; Cummings et al., 2010c; Schauer et al., 2012; Sjöström et al., 2004). However, the mechanisms (beyond body weight reduction) responsible for these effects remain undefined. Although gastric restriction and malabsorption probably contribute to maintenance of long-term weight loss, there is increased interest in the role of endocrine and metabolite changes in the effects of bariatric surgery to induce weight loss and prevent diabetes onset (Scott and Batterham, 2011; Thaler and Cummings, 2009). In particular, post-operative elevations in circulating bile acids have become an increasingly cited mechanism for the metabolic benefits of bariatric surgeries, such as RYGB and vertical sleeve gastrectomy (Cummings et al., 2012; Patti et al., 2009; Thaler and Cummings, 2009). RYGB produces several post-operative alterations in normal GI anatomy and function, such as reduction in gastric volume, bypass of the proximal small intestine and increased flux of incompletely absorbed nutrients and bile into the distal small intestine. By contrast, ileal interposition (IT) surgery only involves transposition of a segment of distal small intestine into the proximal jejunum. Thus, the only major change produced by this surgery is increased flux of incompletely absorbed nutrients and bile to the distal small intestine (Strader, 2006). By investigating the effects of only one of the anatomical alterations produced by RYGB in isolation, we can better assess mechanisms by which this component of bariatric surgery improves glucose metabolism.

Plasma bile acids are elevated after bariatric surgeries such as RYGB and IT surgery in rodents and clinical studies in humans and have been suggested to have a role in producing the metabolic benefits observed after these types of bariatric surgery (Kohli et al., 2010; Nakatani et al., 2009; Patti et al., 2009). However, the mechanisms by which post-operative increases in circulating bile acid concentrations contribute to the metabolic benefits of bariatric

[1]Department of Molecular Biosciences, School of Veterinary Medicine, University of California Davis, Davis, CA 95616, USA
[2]Department of Nutrition, University of California Davis, Davis, CA 95616, USA
[3]Core for Applied Genomics and Ecology (CAGE), University of Nebraska-Lincoln, Department of Food Science and Technology, 323 FIC, Lincoln, NE 68583-0919, USA
[4]Medical Investigators for Developmental Disorders Institute (MIND), University of California Davis, Davis, CA 95616, USA.
[5]Gubra ApS, 2970 Hørsholm, Denmark
[6]Lilly Research Laboratories, Eli Lilly and Company, Lilly Corporate Center, Indianapolis, IN 46285, USA
*Author for correspondence (bpcummings@ucdavis.edu)

Disease Models & Mechanisms • DMM

TRANSLATIONAL IMPACT

Clinical issue
The global prevalence of obesity and type 2 diabetes is increasing at an alarming rate. Bariatric surgery is the most effective treatment for obesity and type 2 diabetes, but the mechanisms responsible are incompletely understood. Circulating bile acid concentrations are elevated after several types of bariatric surgery, and it has been suggested that the increase in bile acids contributes to the metabolic benefits. However, the mechanistic contributions of increased circulating bile acids to the beneficial effects of bariatric surgery remain undefined

Results
In this study, the authors addressed this issue in a novel rat model of type 2 diabetes. After ileal interposition (IT) surgery, improvements in glucose tolerance and β-cell mass coincided with the amelioration of ER stress signaling in liver, adipose and pancreas tissues in this model, independently of body weight changes. Moreover, non-conjugated cholic acid concentrations were preferentially increased after IT surgery in pre-diabetic rats. Finally, incubation of cultured hepatocytes, white adipocytes and β-cells with cholic acid protected all of these cells against the development of ER stress.

Implications and future directions
These results suggest that increases in circulating cholic acid concentrations after IT surgery contribute to improvements in glucose metabolism by decreasing ER stress. This effect of bariatric surgery on ER stress represents a previously unrecognized mechanism by which increases in circulating bile acids after bariatric surgery improve glucose homeostasis. These results advance our understanding of the metabolic benefits of bariatric surgery and suggest that targeting bile acid metabolism could be useful in both the treatment and prevention of type 2 diabetes.

surgery have not been demonstrated. Potential mechanisms by which increases in circulating bile acid concentrations could improve glucose homeostasis include signaling through the membrane-bound G-protein-coupled receptor, TGR5, and the nuclear receptor, FXR. Bile acid signaling through TGR5 receptors on brown adipose tissue increases energy expenditure (Watanabe et al., 2006). Furthermore, bile acid signaling through hepatic FXR decreases hepatic gluconeogenesis and lipogenesis (Thomas et al., 2008).

Another potential mechanism by which post-operative increases in circulating bile acids could improve glucose homeostasis is through amelioration of endoplasmic reticulum (ER) stress in peripheral insulin-sensitive tissues. ER stress has been shown to play an integral role in the development of insulin resistance and diabetes (Ozcan et al., 2004) and administration of tauroursodeoxycholic acid (TUDCA) has been shown to decrease ER stress and improve insulin sensitivity in a mouse model of obesity (Ozcan et al., 2006). However, the effect of other sub-types of bile acids on ER stress has not been previously investigated. Therefore, we hypothesized that bile acids, other than TUDCA, that are increased after bariatric surgery might act to decrease ER stress. ER stress occurs when the folding capacity of the ER is exceeded and unfolded or misfolded proteins accumulate, leading to the unfolded protein response (UPR). The UPR is triggered by transmembrane sensors that detect unfolded proteins in the ER. These proteins are: PKR-like ER kinase (PERK), inositol-requiring enzyme 1α (IRE1α) and activating transcription factor 6 (ATF6) (Hotamisligil, 2010). Activation of PERK results in phosphorylation and inactivation of eukaryotic translation inhibition factor 2α (eIF2α), which inhibits protein synthesis. The UPR also upregulates the synthesis of chaperone proteins, such as binding immunoglobulin protein (BiP), to assist with the increased misfolded protein load (Ron and Walter, 2007). One previous study reported attenuation of ER stress in liver and adipose tissue after weight loss induced by RYGB in humans (Gregor et al., 2009). However, the effect of any type of bariatric surgery, independently of body weight loss, on markers of ER stress has not been previously investigated.

Because the mechanisms by which post-operative increases in circulating bile acids contribute to the improvements in glucose homeostasis after bariatric surgery are undefined, the primary goal of this study was to investigate one potential contributing mechanism. In particular, we focused on the interaction between post-operative increases in circulating bile acids and ER stress signaling. Our previous study of IT surgery in pre-diabetic UCD-T2DM rats demonstrated that IT surgery delays diabetes onset by 4 months (equivalent to ~10 years in a human life-span) and increases total circulating bile acids, independently of changes in food intake or body weight (Cummings et al., 2010c). The UCD-T2DM rat model of type 2 diabetes develops adult-onset polygenic obesity, insulin resistance and marked hyperglycemia, without a defect in leptin signaling (Cummings et al., 2008). Therefore, use of the UCD-T2DM rat model in combination with the IT surgical model is ideal for study of mechanisms by which post-operative increases in circulating bile acid concentrations improve glucose and lipid metabolism in type 2 diabetes.

RESULTS

IT surgery increases diabetes-free days and energy expenditure
Male UCD-T2DM rats underwent surgery at 2 months of age and were studied for either 1.5 (short-term study) or 4.5 months (long-term study). As expected from our previous study (Cummings et al., 2010c), in the long-term study, the average number of diabetes-free days was greater in the IT-operated group (191±5 days) than in control and sham-operated animals (control=166±11 days, sham=172±7 days; $P<0.05$). IT surgery also decreased diabetes incidence in the long-term study such that incidence was 38% in IT-operated animals and 62% and 69% in control and sham-operated animals, respectively. No animals in the short-term study developed diabetes. Correspondingly, glycosylated hemoglobin (HbA$_{1c}$), fasting plasma glucose, insulin, homeostatic model assessment of insulin resistance (HOMA-IR) and triglyceride (TG) concentrations were lower and glucagon-like peptide-1 (GLP-1) was higher in IT-operated animals than in controls ($P<0.05$) (supplementary material Table S1). Food intake and body weight did not differ significantly between groups (Fig. 1A,B).

Energy expenditure was ~4% higher in IT-operated animals compared with control and sham-operated animals during the dark cycle at 1.5 months after surgery ($P<0.05$) (Fig. 1C,D). However, total locomotor activity did not differ between groups (Fig. 1E,F). Thus, the increase in energy expenditure appears to be mediated by increased thermogenesis, rather than by increased physical activity.

IT surgery improves glucose metabolism and preserves β-cell mass
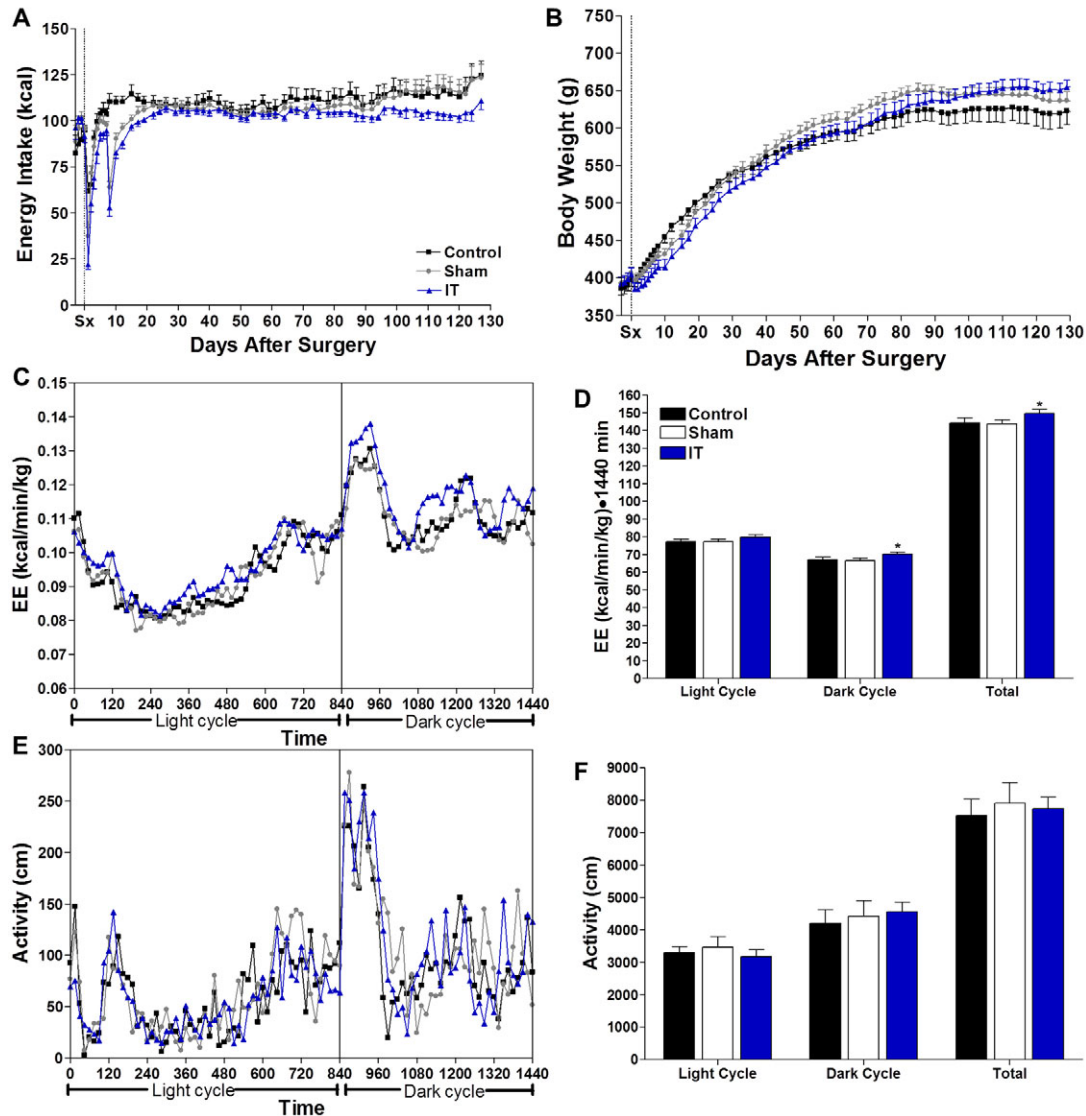We previously reported that IT surgery improved glucose tolerance, glucose-stimulated insulin secretion (GSIS) and

Fig. 1. IT surgery does not affect food intake or body weight, but increases energy expenditure. Energy intake (A), body weight (B), energy expenditure (C), energy expenditure AUC (D), total physical activity (E) and sum of total physical activity (F) in control (n=16), sham (n=16) and IT-operated (n=16) animals. *P<0.05 compared with control and sham by Student's t-test.

nutrient-stimulated GLP-1 secretion at 1 month after surgery (Cummings et al., 2010c). In order to assess the preservation of these improvements over time, serial oral glucose tolerance tests (OGTTs) were performed at 1, 3 and 4 months after surgery. An oral fat tolerance test (OFTT) was performed at 2 months after surgery. Glucose excursions during all three OGTTs were lower in IT-operated animals compared with control and sham-operated animals (P<0.01), except at 3 months where glucose excursions in IT-operated animals were only significantly lower compared with non-operated control animals (P<0.05) (Fig. 2A-C). During the 1 month OGTT, insulin values were significantly lower in IT-operated animals compared with control and sham-operated animals at multiple time points, suggesting an improvement in insulin sensitivity (P<0.01) (Fig. 2D). The increase in plasma insulin concentrations from fasting to peak values was about

twofold greater in IT-operated animals than in control and sham-operated animals during all 3 OGTTs (P<0.01) (Fig. 2D-F), demonstrating an improvement in GSIS after IT surgery (supplementary material Table S2).

Total GLP-1 secretion was fourfold greater in IT-operated animals at 1 and 4 months after surgery compared with control and sham-operated animals (P<0.001) (Fig. 2G-H). Furthermore, the GLP-1 area under the curve (AUC) in IT-operated animals at 4 months after surgery was 39% greater compared with the GLP-1 AUC at 1 month after surgery (P<0.05). Thus, nutrient-stimulated GLP-1 secretion appears to increase over time after IT surgery in UCD-T2DM rats. Similar to previous work, nutrient-stimulated glucose-dependent insulinotropic polypeptide secretion did not differ between groups during the OGTT at 3 months after surgery (Fig. 2I), whereas nutrient-
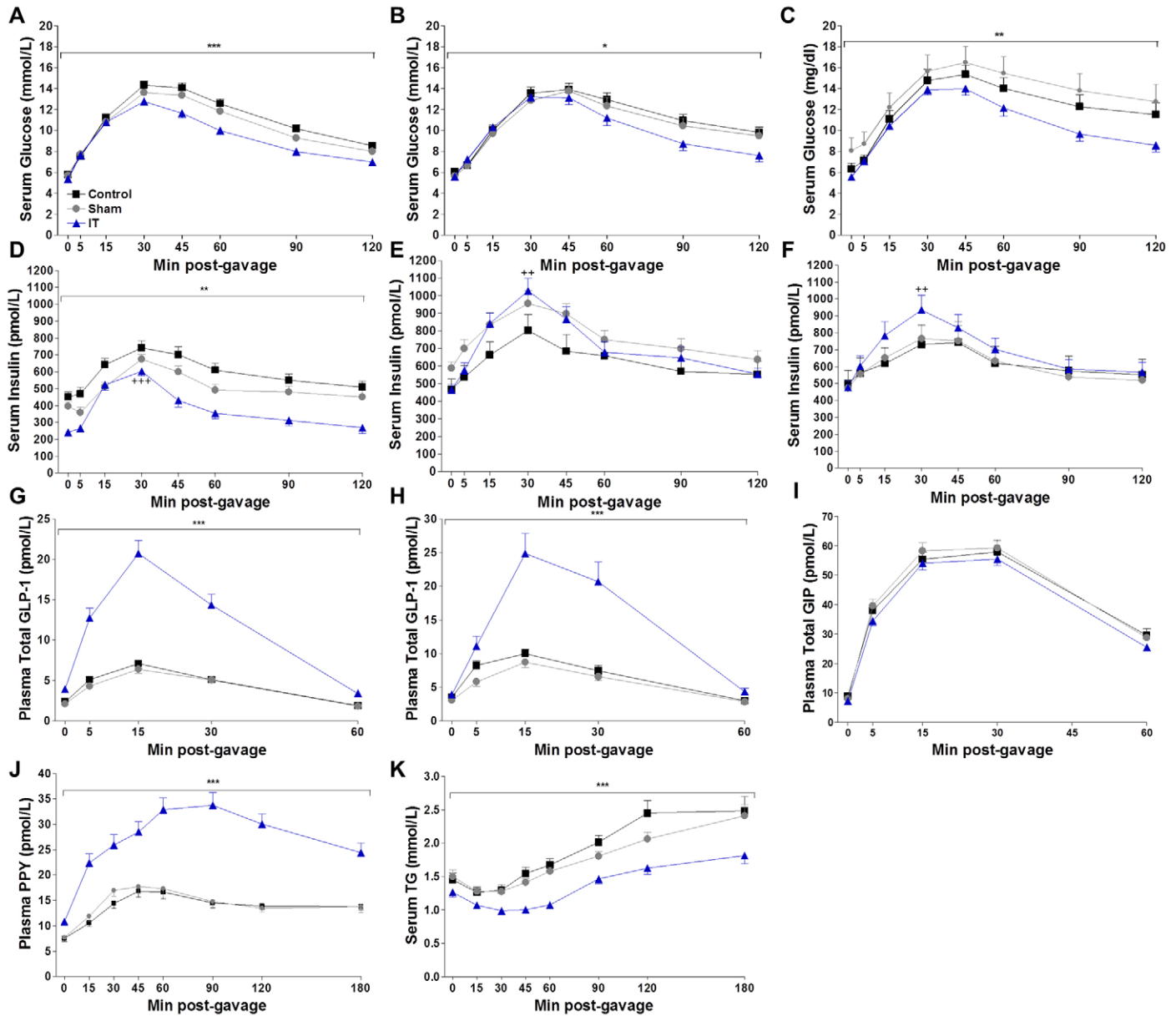
Fig. 2. IT surgery improves glucose tolerance, islet function and nutrient-stimulated GLP-1 secretion. (A-C) Circulating glucose concentrations during OGTTs at 1 (A), 3 (B) and 4 (C) months after surgery. (D-F) Circulating insulin concentrations during OGTTs at 1 (D), 3 (E) and 4 (F) months after surgery. (G,H) Circulating GLP-1 concentrations during OGTTs at 1 (G) and 4 (H) months after surgery. (I) Circulating GIP concentrations during the OGTT at 3 months after surgery. (J,K) Circulating PYY (J) and TG concentrations (K) during the OFTT at 2 months after surgery. During the first month OGTT, *n*=28 per group. During the third and fourth month OGTTs and second month OFTT, *n*= 16 per group. **$P<0.01$, ***$P<0.001$ for IT compared with control and sham by Student's *t*-test of the AUC. *$P<0.05$ for IT compared with control by Student's *t*-test of the AUC. ++$P<0.01$, +++$P<0.001$ for IT compared with control and sham by Student's *t*-test of the percentage change from fasting to peak insulin values.

stimulated peptide YY secretion was markedly elevated in IT-operated animals during the OFTT at 2 months after surgery ($P<0.05$) (Fig. 2J) (Cummings et al., 2010c).

To investigate the molecular basis for enhanced insulin sensitivity in IT-operated animals, we analyzed downstream components of insulin signaling pathways in peripheral tissues of fasted control, sham and IT-operated animals at 1.5 and 4.5 months after surgery. Protein kinase B (Akt) (Ser473) and mitogen-activated protein kinase (MAPK) (Thr202/Tyr204) phosphorylation, normalized to

their protein expression, were two- to threefold higher in liver, skeletal muscle, mesenteric adipose and pancreas in IT-operated animals compared with control animals ($P<0.05$) (Fig. 3). Furthermore, c-Jun N-terminal kinase (JNK) (Thr183/Tyr185) phosphorylation was reduced in liver, skeletal muscle, mesenteric adipose and pancreas tissues in IT-operated animals compared with controls at 4.5 months after surgery ($P<0.05$) (Fig. 3). These results are consistent with an improvement in insulin signaling after IT surgery.
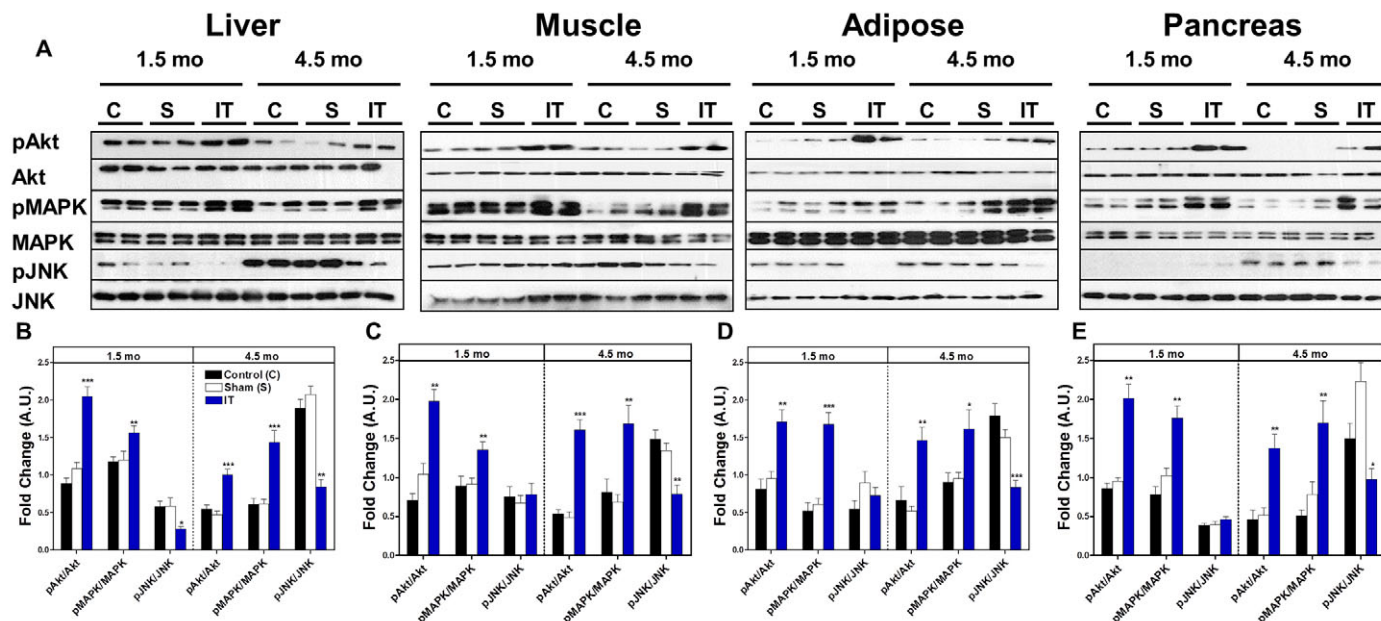
Fig. 3. IT surgery improves insulin signaling in liver, skeletal muscle, mesenteric adipose and pancreas. (A) Representative immunoblots for pAkt (Ser473), total Akt, pMAPK(Thr202/Tyr204), total MAPK, pJNK(Thr183/Tyr185) and total JNK in liver, adipose, skeletal muscle and pancreas at 1.5 and 4.5 months after surgery. (B-E) Results were quantified in densitromic units and expressed relative to the total protein of interest in liver (B), skeletal muscle (C), mesenteric adipose (D) and pancreas (E). *$P<0.05$, **$P<0.01$, ***$P<0.001$ for IT compared with control and sham by Student's t-test; $n=12$ per group at 1.5 months and $n=16$ per group at 4.5 months.

Based on the observed improvement in GSIS, we hypothesized that there might be a related preservation of pancreatic β-cell mass in IT-operated animals. β-cell mass was quantified at 1.5 and 4.5 months after surgery in order to assess temporal changes. At 1.5 months after surgery, islets appeared smaller and β-cell mass was lower in IT-operated animals compared with control and sham-operated animals ($P<0.05$) (Fig. 4A-C,G). At 4.5 months after surgery, islets in IT-operated animals appeared to have better preservation of islet architecture, and β-cell mass was higher in IT-operated animals compared with sham-operated animals ($P<0.05$) (Fig. 4D-G).

IT surgery improves lipid metabolism

During the OFTT at 2 months after surgery, TG excursions were 65% lower in IT-operated animals compared with control and sham-operated animals, suggesting an improvement in lipid clearance ($P<0.001$) (Fig. 2K). Furthermore, skeletal muscle and hepatic ectopic lipid deposition were decreased in IT-operated animals compared with control animals at 1.5 months after surgery (supplementary material Table S1). However, at 4.5 months after surgery this difference was no longer present (supplementary material Table S1). This was probably due to the development of diabetes in control and sham-operated animals and subsequent utilization of body lipids for energy at 4.5 months, resulting in lower ectopic TG deposition. Indeed, we have previously reported that the progression of diabetes in the UCD-T2DM rat is associated with decreases in adiposity and ectopic lipid deposition (Cummings et al., 2008). Similarly, total white adipose tissue mass was significantly reduced in IT-operated animals at 1.5 months after

surgery, but not at 4.5 months after surgery (supplementary material Table S3).

IT surgery increases total circulating bile acids

We and others have reported that circulating bile acid concentrations are increased after IT surgery (Cummings et al., 2010c; Kohli et al., 2010). In order to assess these changes in detail, we determined fasting plasma bile acid profiles at 2 months after surgery (Fig. 5A-C). Total fasting plasma bile acid concentrations and all major bile acid sub-types were increased in IT-operated animals compared with control and sham-operated animals ($P<0.001$) (Fig. 5D). However, when expressed as a percentage of total bile acids, bile acid pools in IT-operated animals had proportionally greater cholic acid and proportionally lower muricholates and deoxycholates ($P<0.05$) (Fig. 5A-C). Similarly, absolute concentrations of both primary and secondary bile acid concentrations were elevated in IT-operated animals ($P<0.001$) (Fig. 5E); however, only primary bile acids were significantly increased as a proportion of the total bile acid pool in IT-operated animals compared with controls ($P<0.05$). Circulating non-conjugated bile acid and non-conjugated cholic acid concentrations were increased in IT-operated animals compared with controls when expressed as an absolute value or as a percentage of the total bile acid pool ($P<0.01$) (Fig. 5A-C,E). Thus, there was a preferential increase in circulating non-conjugated cholic acid in IT-operated animals. However, hepatic total bile acid content and hepatic total cholic acid content did not differ significantly between groups (Fig. 5F), suggesting that the increase in circulating total bile acids in IT-operated animals was unlikely to be due to increased hepatic bile
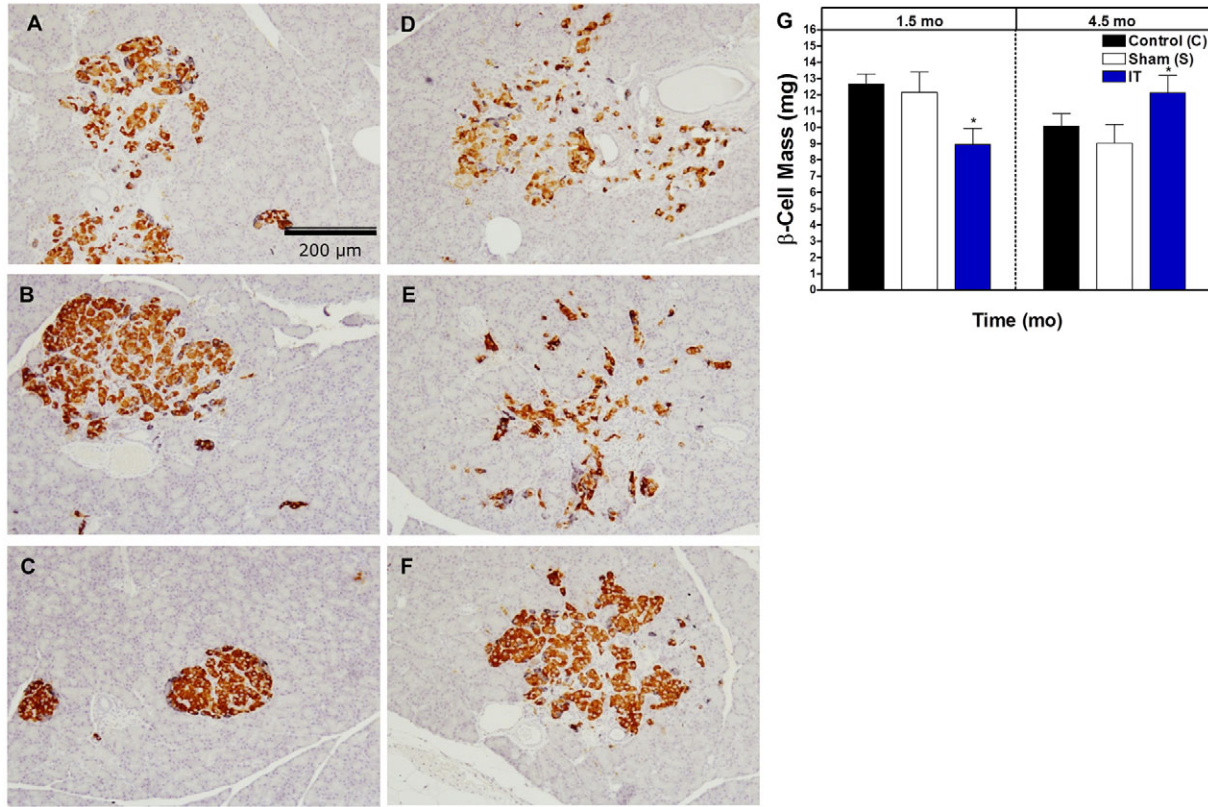
Fig. 4. IT surgery preserves β-cell mass. (A-F) Representative images of pancreas sections immunostained for insulin from pre-diabetic control (A), sham (B) and IT-operated animals (C) at 1.5 months after surgery and control (D), sham (E) and IT-operated animals (F) at 4.5 months after surgery. (G) β-cell quantification in a subset of samples from control (*n*=6), sham (*n*= 6) and IT-operated animals (*n*=6) at 1.5 months after surgery and control (*n*=6), sham (*n*=7) and IT-operated animals (*n*=8) at 4.5 months after surgery. *$P<0.05$, **$P<0.01$ for IT compared with control and sham by Student's *t*-test.

acid production. Cecal total bile acid concentrations were significantly lower in IT-operated animals compared with sham-operated animals ($P<0.05$); however, this difference did not reach significance when compared with the control group (Fig. 5G). This intestinal content sample was collected after an overnight fast, which might have blunted the difference in intestinal bile acid content between the IT-operated and control groups.

Fasting plasma glycine-conjugated bile acid concentrations were elevated in IT-operated animals compared with controls when expressed as either an absolute value or as a percentage of the total bile acid pool ($P<0.001$) (Fig. 5H,I). Furthermore, glycine-conjugated bile acids were also increased in the liver of IT-operated animals compared with controls as both an absolute value and as a percentage of the total hepatic bile acid pool ($P<0.001$) (Fig. 5J). These data coincide with previously published data on bile acid profiles after IT surgery (Kohli et al., 2010) and suggest a shift in hepatic bile acid metabolism, possibly due a change in taurine availability.

Elevations in circulating bile acids might improve glucose and lipid metabolism via activation of FXR. Therefore, the expression of hepatic genes involved in this pathway were investigated by real-time PCR (rtPCR). Although the gene expression of hepatic sterol regulatory element-binding protein 1c (SREBP1c) and cholesterol 7 α-hydrolase (CYP7a1) tended to be decreased in IT-operated

animals; sodium/bile acid co-transporter (SLC10a1), CYP7a1, sterol 12 α-hydrolase (CYP8b1), liver receptor homolog 1 (LRH-1), small heterodimeric partner (SHP), bile acyl-CoA synthetase (SLC27a5) and SREBPc1 did not differ between groups, indicating that the FXR signaling pathway was not significantly engaged following IT surgery (Fig. 5K).

Because the gut microbiome is known to play an important role in bile acid metabolism, gut microbial populations were assessed from intestinal content samples collected from the cecum by pyrosequencing at 4.5 months after surgery. Specifically, proportions of bacterial phyla did not differ between groups (Fig. 6A). However, similar to previous results reported in humans after RYGB, *Gammaproteobacteria* were elevated twofold in IT-operated animals compared with controls ($P<0.05$) (Fig. 6B) (Zhang et al., 2009). At the genus level, *Escherichia* was elevated in IT-operated animals ($P<0.05$) (Fig. 6C).

IT surgery decreases ER stress
Based on the marked improvements of glucose homeostasis and insulin signaling, we hypothesized that IT surgery might contribute to these effects through a decrease in ER stress signaling. Therefore, we assessed activation of the three sub-arms of ER stress signaling. Immunoblot analysis of liver, adipose and pancreas lysates revealed that phosphorylation of PERK (Thr980),
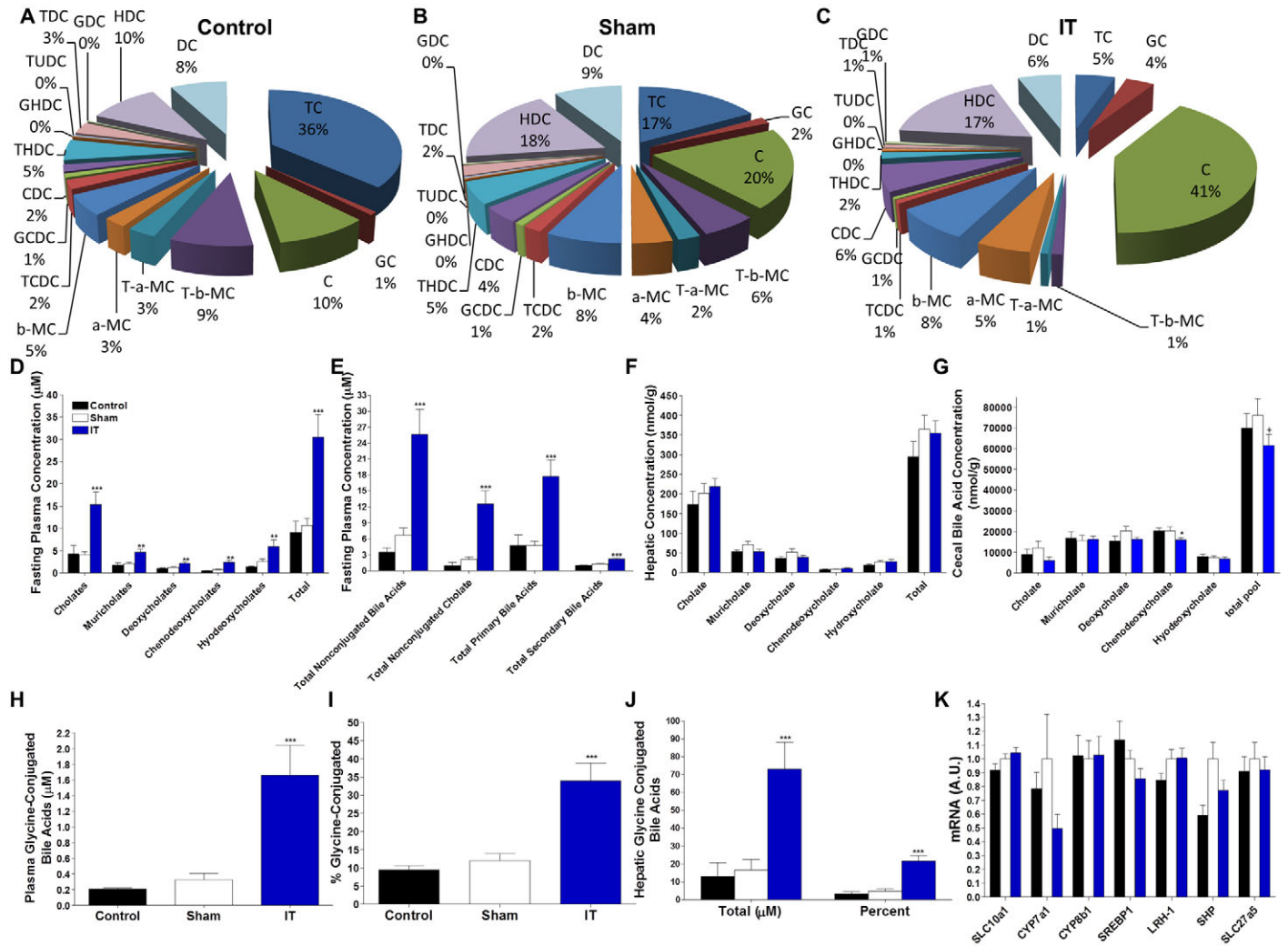
Fig. 5. IT surgery preferentially increases nonconjugated primary bile acids. (A-C) Fasting plasma bile acid profiles in control (A), sham (B) and IT-operated animals (C) at 2 months after surgery. (D) Fasting plasma bile acid concentrations. (E) Fasting plasma non-conjugated bile acid, non-conjugated cholic acid, primary bile acid and secondary bile acid concentrations. (F) Hepatic bile acid profiles. (G) Bile acid profiles in cecal contents. (H) Fasting plasma glycine-conjugated bile acid concentrations. (I) Fasting plasma glycine-conjugated bile acid concentrations expressed as a percentage of conjugated bile acids. (J) Hepatic glycine-conjugated bile acid concentrations expressed as an absolute value and as a percentage of the total hepatic bile acid pool. (K) Hepatic mRNA expression of genes involved in bile acid metabolism and the FXR pathway relative to *ARBP*. All plasma values were measured at 2 months after surgery. Liver and cecal contents values were measured at 4.5 months after surgery; n=16 per group. *$P<0.05$, **$P<0.01$, ***$P<0.001$ for IT compared with control and sham, [+]$P<0.05$ compared with sham by Student's *t*-test. C, cholate; CDC, chenodeoxycholate; DCA, deoxycholate; GC, glycocholate; GCDC, glycochenodeoxycholate; GDC, glycodeoxycholate; GHDC, glycohyodeoxycholate; HDC, hyodeoxycholate; T-a-MC, tauro-α-muricholate; T-b-MC, tauro-β-muricholate; TC, taurocholate; TCDC, taurochenodeoxycholate; TDC, taurodeoxycholate; THDC, taurohyodeoxycholate; TTHC, taurotetrahyodeoxycholate; TUDC, tauroursodeoxycholate.

eIF2α (Ser51) and IRE1α (Ser724) and expression of X-box binding protein-1 (sXBP1), ATF6 and BiP protein were reduced in IT-operated animals compared with sham and control groups at both 1.5 and 4.5 months after surgery ($P<0.05$) (Fig. 7A-B,D-E), except that hepatic BiP expression did not differ between groups at 1.5 months. However, markers of ER stress in skeletal muscle did not differ between groups at 1.5 months after surgery, but were two- to threefold lower in IT-operated animals at 4.5 months after surgery ($P<0.05$) (Fig. 7C).

One of the major mechanisms by which ER stress is proposed to contribute to the development of insulin resistance is through

the promotion of inflammation (Hotamisligil, 2010). Therefore, markers of inflammation, tumor necrosis factor-α (TNF-α) and monocyte chemotactic protein-1 (MCP-1), were measured. At 1.5 months after surgery only TNF-α was reduced in adipose tissue from IT-operated animals ($P<0.05$). However, TNF-α and MCP-1 were markedly reduced in liver, muscle and mesenteric adipose tissue in IT-operated animals compared with controls animals at 4.5 months after surgery ($P<0.05$) (supplementary material Fig. S1). This difference persisted without inclusion of diabetic animals in the analysis, indicating that the effect of IT surgery in reducing markers of inflammation was independent of diabetes.
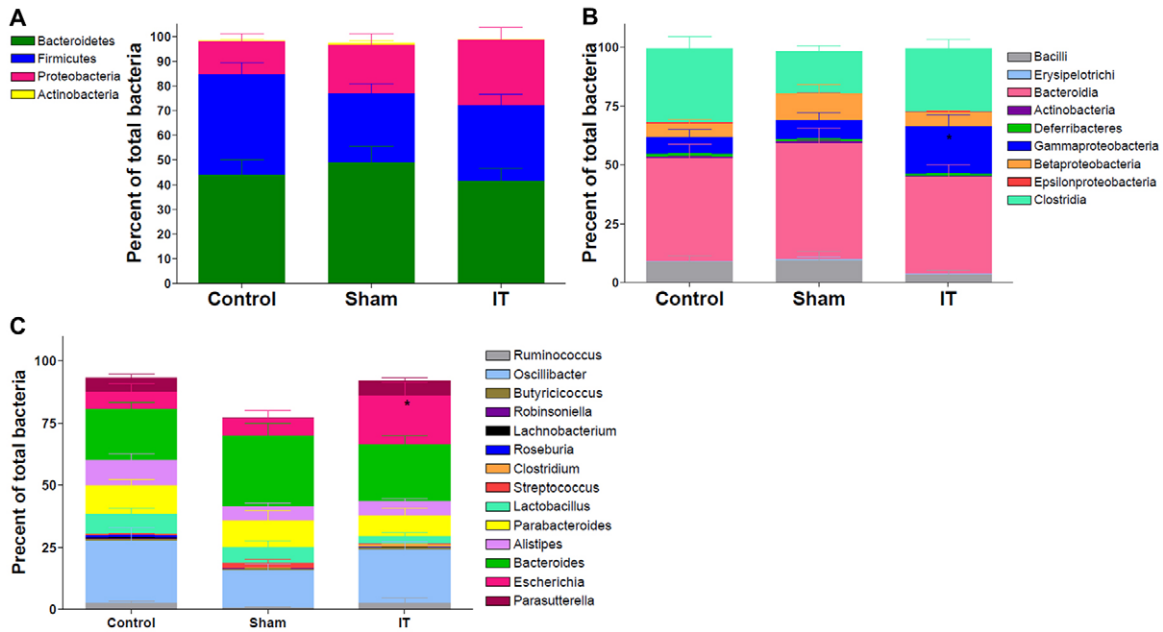
Fig. 6. IT surgery increases the relative expression of *Gammaproteobacteria* in cecal contents. (A) Average phylum-level composition of cecal contents. (B) Average class-level composition of cecal contents. (C) Average genus-level composition of cecal contents. *P<0.05 for IT compared with control and sham by Student's *t*-test; *n*=10-14 per group.

Cholic acid decreases ER stress in liver, adipocyte and β-cell culture

Based on previous work demonstrating that TUDCA decreases ER stress and improves insulin sensitivity (Ozcan et al., 2006), we hypothesized that other bile acids might also ameliorate ER stress. Thus, we tested the effect of cholic acid, the bile acid that was increased by the greatest magnitude after IT surgery, to attenuate ER stress in cultured hepatocytes, adipocytes and β-cells. Cells were incubated for 24 hours in the presence or absence of cholic acid (100 μM). ER stress was induced by treatment with thapsigargin (2 μM) for 2 hours. Thapsigargin treatment resulted in significant increases in markers of the PERK, IRE1α and ATF6 pathways of ER stress in all cell types. Pretreatment of hepatocytes with cholic acid resulted in normalization of markers of the IRE1α and ATF6 pathways of ER stress to control levels (Fig. 8A,B). Pretreatment of adipocytes with cholic acid resulted in reductions of markers of the PERK and IRE1α pathways of ER stress (*P*<0.05) (Fig. 8A,C). Pretreatment of β-cells with cholic acid resulted in reductions of the PERK- and ATF6-mediated pathways of ER stress and reductions of IRE1α (Ser724) phosphorylation but not sXBP1 expression (Fig. 8A,D). In contrast to IT-operated animals, pretreatment of hepatocytes with cholic acid did not affect activation of the PERK pathway of ER stress, and pretreatment of adipocytes with cholic acid did not affect activation of the ATF6 pathway of ER stress. Overall, these results support our hypothesis that cholic acid can improve glucose homeostasis by attenuating ER stress.

DISCUSSION

In this study we demonstrate that IT surgery in pre-diabetic UCD-T2DM rats results in marked improvements in glucose and lipid metabolism, with concurrent increases in circulating bile acids. We also found significant decreases in ER stress signaling in peripheral tissues of IT-operated animals, which probably contributed to the improvements in insulin sensitivity and preservation of β-cell mass. Furthermore, we demonstrate that incubation with cholic acid protects cells from the development of ER stress in hepatocyte, adipocyte and β-cell culture, suggesting that increases in circulating bile acid concentrations might contribute to attenuation of ER stress. Thus, we have identified a potential pathway by which post-operative increases in circulating bile acids might improve metabolic homeostasis after bariatric surgery.

Similar to previous studies, we found that fasting plasma total bile acid concentrations were markedly elevated in IT-operated animals and that IT surgery produced a preferential increase in circulating non-conjugated cholic acid concentrations (Cummings et al., 2010c; Kohli et al., 2010). However, hepatic total bile acid content and hepatic cholic acid content did not differ between groups. These data are consistent with previous reports (Kohli et al., 2010) and support the hypothesis that IT surgery results in an increase in circulating bile acids by increasing reabsorption of bile acids in the transposed ileal segment. However, the gut microbiome has received increasing attention for its role in modulating bile acid metabolism and thus post-operative changes in gut microbial populations might also contribute to post-operative changes in bile acid absorption (Swann et al., 2011). Surprisingly, changes in gut microbial populations after IT surgery were small in comparison to the phyla-level alterations in gut microbiome composition reported after RYGB. Studies in humans and rodents report proportional decreases in *Firmicutes* after RYGB (Li et al., 2011; Zhang et al., 2009), which were not present after IT surgery. However, similarly to RYGB, IT-operated animals exhibited
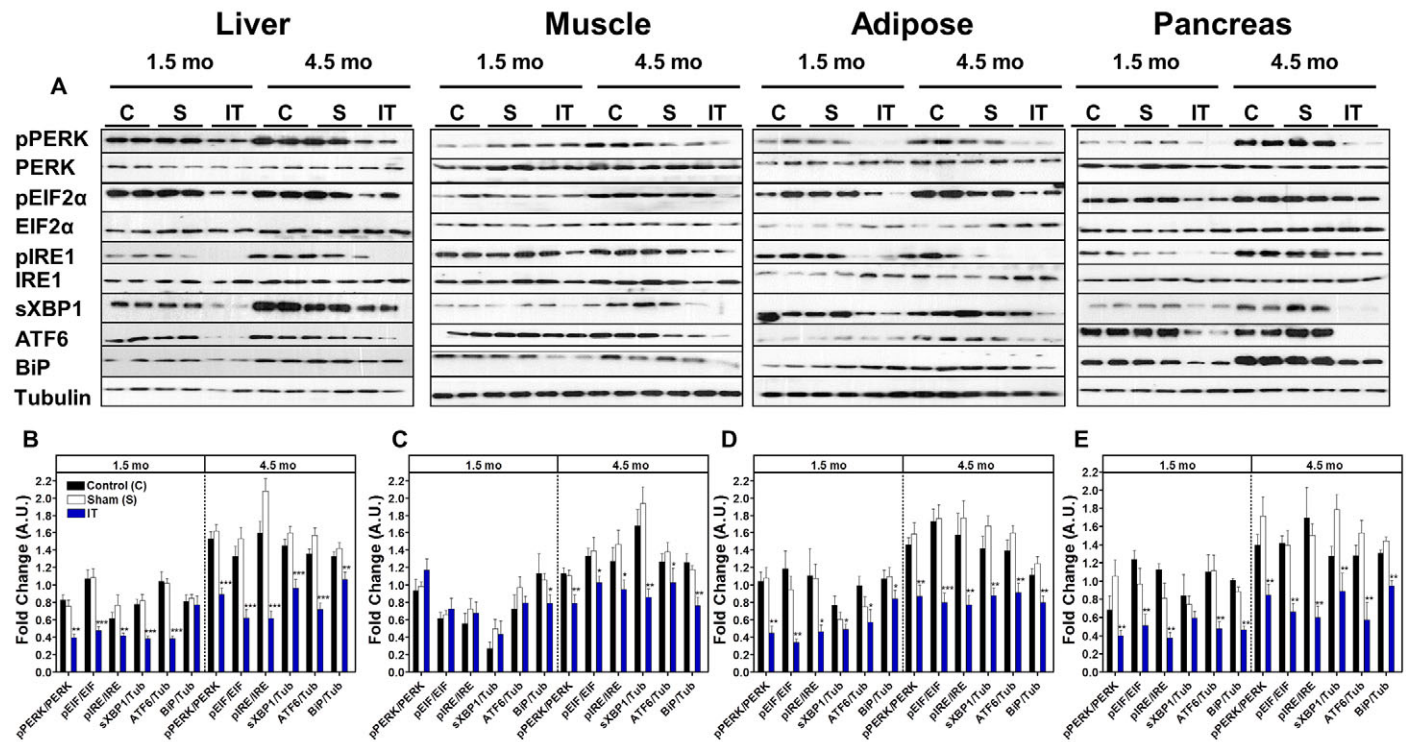
Fig. 7. IT surgery decreases markers of ER stress in liver, adipose, muscle and pancreas. (A) Representative immunoblots for pPERK(Thr980) and total PERK, peIF-2α(Ser51) and total eIF-2α, pIRE1(Ser724) and total IRE1, sXBP1, BiP and tubulin in liver, skeletal muscle, mesenteric adipose and pancreas at 1.5 and 4.5 months after surgery. All blots were scanned and quantified using FluorChem 9900. (B-E) Results were quantified in densitromic units and expressed relative to the total protein of interest or relative to tubulin for BiP, ATF6 and sXBP1 in liver (B), skeletal muscle (C), mesenteric adipose (D) and pancreas (E). *$P<0.05$, **$P<0.01$, ***$P<0.001$ for IT compared with control and sham by Student's t-test; $n=12$ per group at 1.5 months and $n=16$ per group at 4.5 months.

increases in *Gammaproteobacteria* and *Escherichia* (Furet et al., 2010; Li et al., 2011; Zhang et al., 2009). Decreases in intestinal enterobacteria (a member of the class *Gammaproteobacteria*) have been shown to be associated with increases in intestinal bile acid absorption (Miyata et al., 2011). Therefore, the increases in intestinal *Gammaproteobacteria* observed after IT surgery do not appear to be associated with the increases in circulating bile acid concentrations. However, further study on the effect of other members of this class on bile acid absorption is needed.

Increases in circulating bile acids might contribute the metabolic improvements after IT surgery by signaling through TGR5 and FXR. Increased circulating bile acids might contribute to increased energy expenditure because cholic acid administration has been shown to increase energy expenditure by signaling through TGR5 in brown adipose tissue and skeletal muscle (Watanabe et al., 2006). Bile acid administration has also been shown to improve glucose and lipid metabolism by potentiating GLP-1 secretion through TGR5 signaling and by decreasing hepatic gluconeogenesis and lipogenesis through FXR activation (Kalaany and Mangelsdorf, 2006; Pols et al., 2011; Thomas et al., 2009). However, gene expression analysis revealed that indices of hepatic FXR activation did not differ between groups. Furthermore, the decreased luminal bile acid content in IT-operated animals in this study, as well as in another previous study (Kohli et al., 2010), suggests that a contribution of bile acids to the increase in nutrient-stimulated

GLP-1 secretion through direct stimulation of intestinal TGR5 receptors is unlikely.

A previous study reported that administration of TUDCA decreased ER stress and improved insulin sensitivity in obese mice (Ozcan et al., 2006). However, the effect of other bile acid sub-types on ER stress is unknown. Thus, we hypothesized that the increase in circulating bile acid concentrations after IT surgery might have contributed to the improvements of insulin sensitivity and β-cell mass by decreasing ER stress. All three sub-arms of ER stress signaling were decreased in liver, adipose and pancreas of IT-operated animals compared with controls. ER stress signaling was decreased in skeletal muscle at 4.5 months, but not 1.5 months after surgery. Notably, previous studies demonstrated that markers of ER stress are activated in models of obesity in liver and adipose, but not in skeletal muscle (Ozcan et al., 2004). Thus, attenuation of ER stress is a likely contributor to the improvement of insulin sensitivity in these tissues. Attenuation of ER stress in islets might contribute to the preservation of β-cell mass and improvement of insulin secretion in IT-operated animals. We found that β-cell mass was significantly lower at 1.5 months and significantly higher at 4.5 months after surgery in IT-operated animals compared with controls. We hypothesize that this was due to an improvement in insulin sensitivity in IT-operated animals at 1.5 months after surgery, resulting in less islet hypertrophy. At 4.5 months after surgery, we hypothesize that IT-operated animals had become
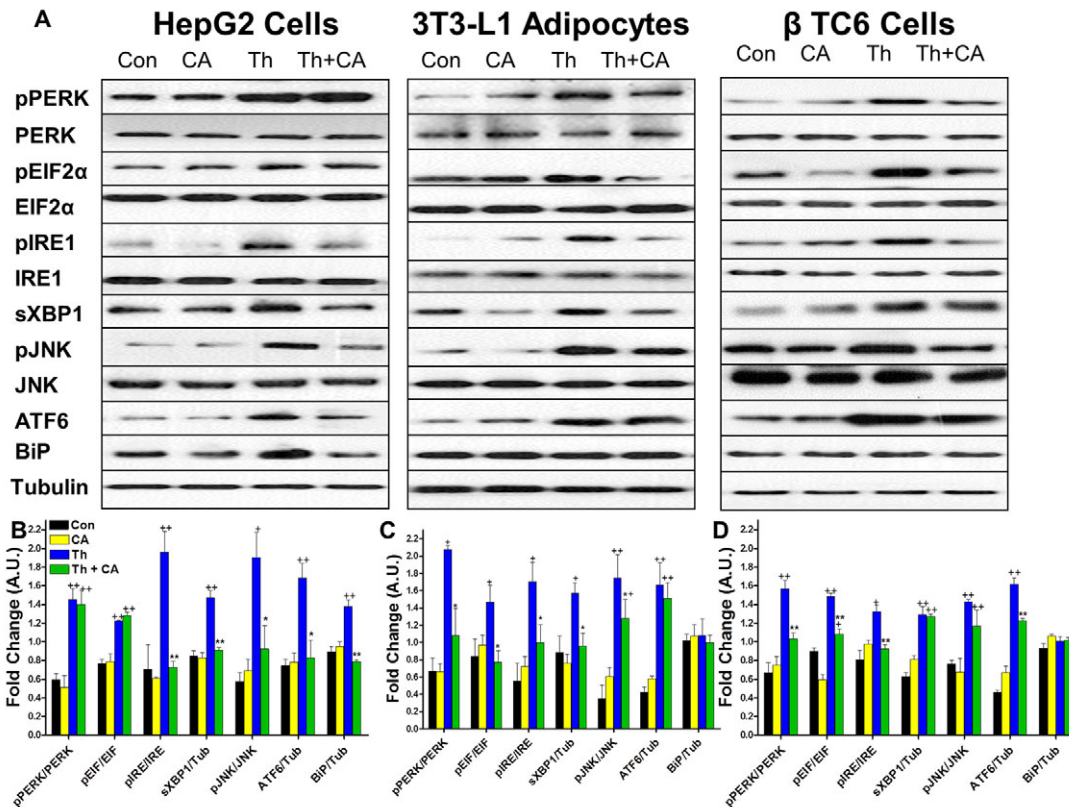
Fig. 8. Preincubation of hepatocytes, adipocytes and β-cells with cholate protects cells from the development of ER stress. Cells were incubated with 100 µM cholic acid or DMSO for 24 hours then exposed to 2 µM thapsigargin for 2 hours. (A) Representative immunoblots for pPERK(Thr980) and total PERK, peIF-2α(Ser51) and total eIF2α, pIRE1(Ser724) and total IRE1, sXBP1, pJNK(Thr183/Tyr185) and total JNK and BiP. Experiments were performed in HepG2, differentiated 3T3 L1 adipocytes and β-TC6 cells. (B-D) Control cells (Con) were not exposed to cholic acid or thapsigargin. Other cells were exposed to chloic acid but not to thapsigargin (CA), to thapsigargin but not cholic acid (Th), or preincubated with cholic acid and then exposed to thapsigargin (Th + CA). Results were quantified in densitromic units and expressed relative to the total protein of interest or relative to tubulin for BiP, ATF6 and sXBP1 in hepatocytes (B), adipocytes (C) and β-cells (D). *P<0.05, **P<0.01 for IT compared with Th by Student's t-test. +P<0.05, ++P<0.01 compared with Con and CA by Student's t-test; n=3 per group.

relatively more insulin resistant, as reflected by the increase in HOMA-IR at this time point, but were able to compensate for this in part through an expansion of β-cell mass. Insulin signaling in the β-cell has been shown to induce β-cell proliferation (Shawl et al., 2009), and ER stress in the β-cell has been implicated in progressive β-cell failure observed in type 2 diabetes (Harding and Ron, 2002). However, because these measurements were made in whole pancreas tissue, it is not possible to localize the decreases of ER stress specifically to the islet component of the pancreas. Nevertheless, preincubation of β-cells, hepatocytes and adipocytes with cholic acid protected cells from the development of ER stress. These results suggest that the increase in circulating cholic acid concentrations in IT-operated animals might have contributed to the reduction of ER stress in peripheral tissues. Further studies are needed to test the effects of other bile acid subtypes that are increased after IT surgery to protect against the development of ER stress in insulin sensitive tissues.

It is important to note that the metabolic benefits of IT surgery are likely not due to increases in circulating bile acid concentrations alone. Increases in nutrient-stimulated GLP-1 secretion in the IT-operated rats also likely contributed to the improvement of glucose homeostasis. GLP-1 has well known effects to increase GSIS, decrease glucagon secretion and improve insulin sensitivity (Baggio and Drucker, 2007; Brubaker and Drucker, 2004). Improvement of GSIS was clearly demonstrated during all 3 OGTTs in which IT-operated animals exhibited about twofold greater GSIS compared with sham-operated and control animals. IT-operated animals exhibited improved insulin sensitivity compared with control and sham-operated animals based on decreased HOMA-IR and increased activation of insulin signaling in liver, skeletal muscle, mesenteric adipose and pancreas. Increases in nutrient-stimulated GLP-1 secretion might contribute to the improvement in insulin sensitivity by decreasing lipotoxicity, which is considered an important contributor to insulin resistance (Morino et al., 2006; Samuel et al., 2010). We have previously reported that administration of a GLP-1 agonist lowers circulating lipids in UCD-T2DM rats (Cummings et al., 2010a). This effect is possibly mediated by increased fatty acid oxidation (Sancho et al., 2006). IT-operated animals exhibited clear reductions in lipotoxicity with lower fasting plasma lipids, increased lipid clearance during the OFTT and decreased ectopic lipid deposition.

Disease Models & Mechanisms ● DMM

In conclusion, we have demonstrated that IT surgery in UCD-T2DM rats delays diabetes onset with concurrent improvements in glucose and lipid metabolism. Increases in GLP-1 probably contribute to the improvements in glucose homeostasis; however, the results from this study also indicate that increases in circulating bile acid concentrations, particularly non-conjugated cholic acid, might contribute to the improvement of insulin sensitivity and islet function by decreasing ER stress. We have, for the first time, demonstrated that both IT surgery and cholic acid decrease ER stress in insulin-sensitive tissues, thus identifying a potential pathway by which post-operative increases in circulating bile acid concentrations might contribute to metabolic improvements following bariatric surgery. Furthermore, these results emphasize the importance of post-operative increases in circulating bile acids in the beneficial metabolic effects of bariatric surgery and the potential utility of targeting bile acid metabolism in the management and prevention of type 2 diabetes.

MATERIALS AND METHODS

Diets and animals
Male UCD-T2DM rats were individually housed in hanging wire cages in the animal facility in the Department of Nutrition at the University of California, Davis and maintained on a 14:10 hour light-dark cycle. Weight-matched animals were placed on study at 2 months of age and either underwent sham or IT surgery or were placed in a non-operated control group. One subset of animals was euthanized at 1.5 months after surgery (short-term study, n=12) and the rest were euthanized at 4.5 months after surgery (long-term study, n=16). Animals were euthanized with an overdose of pentobarbital (200 mg/kg, i.p.) after an overnight fast. Tissues were weighed and flash frozen in liquid nitrogen. Baseline and final fasting blood samples were collected on the day of euthanasia. All animals received ground chow (no. 5012, Ralston Purina, Belmont, CA). Food intake and body weight were measured three times a week. Non-fasting blood glucose was measured weekly with a glucose meter (One-Touch Ultra, LifeScan, Milpitas, CA) at 14:00-16:00 hours. Diabetes onset was defined as a non-fasted blood glucose value >11.1 mmol/l on 2 consecutive weeks. Indirect calorimetry was performed at 1.5 months after surgery using an Accuscan Integra ME System. An OGTT was performed in all animals at 1 month after surgery and then in long-term animals at 3 and 4 months after surgery (1g/kg body weight gavage with dextrose). An OFTT was performed at 2 months after surgery [1.5g/kg body weight gavage with Intralipid (Fresenius Kabi; Uppsala, Swede)]. The experimental protocols were approved by the UC Davis Institutional Animal Care and Use Committee.

IT surgery
IT surgery was performed as previously described (Cummings et al., 2010c). Rats were placed on a liquid diet (Boost, Novartis, Minneapolis, MN) 4 days prior to surgery and for 7 days post-surgery and received enrofloxacin (20 mg/kg/d, s.c.) before and after surgery. Anesthesia was induced and maintained with isoflurane (1–5%). A midline abdominal incision was made and a 10-cm segment of ileum 5-10 cm proximal to the ileocecal valve was isolated and transected. An anastomosis was made with the remaining ends of the ileum using 7-0 PDS suture (Ethicon). Next, a transection was made 5-10 cm distal to the ligament of Treitz.

The isolated ileal segment was then inserted isoperistaltically. Sham-operated animals were treated in the same manner as the IT group. Sham surgeries were performed by making transections in the same locations as in the IT-operated animals and bowel were reattached by anastomosis in their original position.

Hormone and metabolite measurements
Fasting (13 hour) plasma and whole blood samples were collected at baseline and on the day of euthanasia into EDTA-treated tubes. Plasma was assayed for glucose, insulin, triglycerides, cholesterol, adiponectin and glucagon. Plasma glucose, cholesterol and TG were measured using enzymatic colorimetric assays (Thermo DMA Louisville, CO). Adiponectin and PYY were measured using mouse- or rat-specific radioimmunoassay (Millipore, St. Charles, MO). Insulin and GIP were measured by ELISA (Millipore, St Charles, MO). Total GLP-1 was measured by sandwich electrochemiluminescence immunoassay (Meso Scale Discovery; Gaithersburg, MA). HbA$_{1c}$ was measured using an enzymatic colorimetric assay (Diazyme; Poway, CA).

Tissue triglyceride content measurement
Liver and skeletal muscle TG content were measured using the Folch method for lipid extraction followed by spectrophotometric measurement of TG content (Thermo Electron, Louisville, CO) as previously described (Cummings et al., 2010b; Folch et al., 1957).

Islet immunohistochemistry
Whole pancreas samples were fixed in 4% paraformaldehyde. For determination of β-cell mass, 8-10 sections per pancreas were sectioned in a systematic uniform random manner and analyzed as previously described (Paulsen et al., 2010). Immunostaining was performed using a primary non-β-antibody dilution, including mouse anti-glucagon, rabbit anti-somatostatin and rabbit anti-pancreatic polypeptide and a secondary biotinylated antibody mixture (Fab2 fragment donkey anti-mouse at 1:2000 dilution and Fab2 fragment donkey anti-rabbit at 1:2000 dilution). Sections were then blocked for 15 minutes in 10% rabbit normal serum (Dakocytomation #X0902) and incubated overnight at 4°C in guinea pig anti-insulin (Dakocytomation A0564). Sections were eventually developed in NovaRed (Vector Laboratories, SK4800) then stained in a Mayer solution. Stereological estimations were performed on all sections using a Leica DMLB microscope (Leica, Glostrup, Denmark). Systematic uniform random sampling within a section was enabled by using an ECO-Drive microscope stage (Märzhäuser Wetzlar, Wetzlar, Germany) controlled by a computer with WIN-Commander 4.1.3.0 software (Märzhäuser). The applied probes used for the stereological examinations (point-counting grid) were fixed to the table so that the microscope projected the image onto the grid. The pancreas area/volume and β-mass/non-β-mass ratios were estimated with a 144-point grid. The total mass of β-cells was calculated as:

$$M_{\text{beta}} = \frac{\sum P_{\text{beta}}}{256(\sum P_{\text{pan}} + \frac{1}{4}P_{\text{non-pan}})} M_{\text{tis}} \ ,$$

where M_{beta} is the total β-cell mass, $\sum P_{\text{beta}}$ is the total number of points that hit β-cells in all sections, $\sum P_{\text{pan}}$ the number of points hitting pancreas, $\sum P_{\text{non-pan}}$ the number of points hitting non-pancreatic tissue and M_{tis} the wet weight of the removed tissue.

Bile acids profiles

Fasting plasma bile acid profiles were analyzed at 2 months after surgery, as previously described (Bootsma et al., 1999; Torchia et al., 2001). An internal standard mixture of D4-cholate, D4-β-muricholate, D4-α-muricholate, D4-chenodeoxycholate, D4-deoxycholate, D4-hyodeoxycholate, D4-ursodeoxycholate and D4-lithocholate and their tauroconjugated and glycoconjugated counterparts was prepared in acetonitrile. Eluted bile salts were detected by negative ion electrospray mass spectrometry on a linear trap LTQ mass spectrometer (Thermo-Finnigan, San Jose, CA) using a data-dependent stage of detection, triggering a qualitative 0 m/z neutral loss scan at 27% normalized collision energy. Peak areas from initial scans of individual bile salts at 514.3, 498.3, 464.3, 447.3, 411.3, 407.3, 395.3, 393.3 and 391.3 m/z were integrated and the response factors defined by peak area ratios of analytes to that of internal, deuterated standards. The response factors were read against those obtained from standard curves in surrogate matrix, and molar levels of serum or plasma levels were interpolated from standard curves. Response factors for all samples comprised peak area ratios of non-labeled salts normalized to the stable-labeled counterparts. Concentrations were interpolated by linear regression from curves of known standards. Plasma and intestinal perfusates were normalized to volume. Tissue bile salts were normalized to tissue dry weight for calculations of total concentration. Percentages were normalized to total mass of all bile salts detected.

rtPCR

RNA isolation from tissue and real-time PCR was performed according to the manufacturer's instructions using ABI Prism 6100 and ABI 7100 systems with assays on demand (Applied Biosystems, Carlsbad, CA). Briefly, samples were lysed in 2× Nucleic Acid Purification Lysis Solution (Applied Biosystems). Samples were homogenized for 30 seconds and then treated with a proteinase K solution and allowed to incubate for 1 hour under ambient conditions. RNA was isolated on the ABI 6100 system and assessed by agarose gel electrophoresis. Total RNA samples were diluted (1:20), in RNase-free water. cDNA was generated using the ABI High Capacity cDNA reverse transcription kit (Applied Biosystems). Individual probes were obtained from ABI (Assays on demand) for the genes *ASBT, ARBP, CYP7A1, CYP8B1, FGF15, IBABP, LRH-1, SHP, SL10A1, SLC10A2, SLC27A5* and *SREPB1c*. These were mixed with diluted cDNA, cofactors and substrates and processed on the ABI 7100 system. The signals were normalized to that of the housekeeping gene *ARBP*.

Cecal microbiota

The cecal contents of animals euthanized at 4.5 months after surgery were collected for analysis of microbial populations by pyrosequencing performed by the Core for Applied Genomics and Ecology (CAGE, University of Nebraska) using a Roche Genome Sequencer GS-FLX. DNA was extracted using the QiaXtractor (Qiagen, Valencia, CA). The V1-V2 region of the 16S rRNA gene was amplified using bar-coded fusion primers with the Roche-454 A or B Titanium sequencing adapters. The PCR mixture contained 1 ml of forward primer mix, 1 ml of reverse primer, 0.25 ml of Ex-Taq polymerase (TaKaRa Bio, Clontech Laboratories, Mountain View, CA), 1.5 ml of the sample, 6.25 ml of Ex-Taq buffer, 5 ml of deoxynucleotides and 37 ml of sterile distilled H_2O. The PCR program consisted of an initial denaturing step for 5 minutes at 95°C, followed by 30 cycles of denaturation at 95°C for 45 seconds, annealing at 57°C for 45 seconds and extension at 72°C for 2 minutes, with a final step at 72°C for 10 minutes. The PCR products were quantified on the basis of their staining intensity using the image acquisition software Genesnap (Syngene USA). PCR products were combined in equal amounts and gel-purified using the QIAquick Gel Extraction Kit (Qiagen, USA). Pyrosequencing was performed from the A end with the 454/Roche A sequencing primer kit using a Roche Genome Sequencer GS-FLX following the manufacturer's protocol. Filter-pass reads were parsed into sample-barcoded bins and uploaded to a publicly accessible MySQL database (http://cage.unl.edu). Reads were assigned taxonomic status with a parallelized version of the multi-CLASSIFIER algorithm. Reads in each taxonomic bin were normalized as the absolute proportion of the total number of reads for each sample. Discriminant analysis was performed using a multi-sample classifier downloaded from Ribosomal Database Project (RDP; http://rdp.cme.msu.edu/).

Immunoblotting

Tissues were ground in liquid nitrogen and lysed using radio-immunoprecipitation assay (RIPA) buffer (150 mM NaCl, 1.0% IGEPAL CA-630, 0.5% sodium deoxycholate, 0.1% SDS, and 50 mM Tris pH 7.4, 5 mM EDTA, 1 mM NaF, 1 mM sodium orthovanadate and protease inhibitors). Lysates were clarified by centrifugation at 10,000 r.p.m. (9600 g) for 10 minutes and protein concentrations determined using a bicinchoninic acid protein assay kit (Pierce Chemical, IL). Proteins were resolved by SDS-PAGE and transferred to nitrocellulose membranes. Immunoblots were performed with the indicated antibodies (supplementary material Table S4). Proteins were visualized using enhanced chemiluminescence (ECL; Amersham Biosciences) and the pixel intensities of immunoreactive bands quantified using FluorChem 9900 (Alpha Innotech, CA).

Cell culture

HepG2 cells were maintained in culture in a humidified 5% CO_2 atmosphere at 37°C in complete medium consisting of regular Delbecco's modified Eagle's medium (DMEM) supplemented with 10% fetal bovine serum (FBS), 100 units/ml penicillin and 100 µg/ml streptomycin. 3T3-L1 cells were maintained in high glucose (25 mM) DMEM supplemented with 10% newborn calf serum and penicillin-streptomycin. When confluent (designated day 0), cells were switched to high insulin (1.7 µM), high glucose DMEM supplemented 10% FBS. Differentiation of 3T3-L1 pre-adipocytes was induced at day 2 by switching to high insulin, high glucose DMEM supplemented with 10% FBS, 1 µM dexamethasone, and 0.5 mM 3-isobutyl-l-methylxanthine. After 48 hours, the medium was switched back to high insulin, high glucose DMEM supplemented 10% FBS. β-TC6 insulinoma cells (ATCC: CRL-11506) were cultured in DMEM containing 25 mM glucose, 15% FBS, 50 U/ml penicillin and 50 µg/ml streptomycin and maintained in a CO_2 incubator (8% CO_2) at 37°C. ER stress was induced in cells by treatment with thapsigargin (2 µM) for 2 hours.

Statistics and data analyses

All statistical analyses were performed using GraphPad Prism 4.00 for Windows (GraphPad Software, San Diego, CA). Data were analyzed by two-factor repeated measures ANOVA with Bonferroni's post-test or Student's t-test where appropriate. Differences were considered significant at $P < 0.05$. Data are expressed as mean ± s.e.m.

SUPPLEMENTARY MATERIAL
Supplementary material for this article is available at
http://dmm.biologists.org/lookup/suppl/doi:10.1242/dmm.010421/-/DC1

REFERENCES

Baggio, L. L. and Drucker, D. J. (2007). Biology of incretins: GLP-1 and GIP. *Gastroenterology* **132**, 2131-2157.

Bootsma, A. H., Overmars, H., van Rooij, A., van Lint, A. E., Wanders, R. J., van Gennip, A. H. and Vreken, P. (1999). Rapid analysis of conjugated bile acids in plasma using electrospray tandem mass spectrometry: application for selective screening of peroxisomal disorders. *J. Inherit. Metab. Dis.* **22**, 307-310.

Brubaker, P. L. and Drucker, D. J. (2004). Minireview: Glucagon-like peptides regulate cell proliferation and apoptosis in the pancreas, gut, and central nervous system. *Endocrinology* **145**, 2653-2659.

Buchwald, H., Avidor, Y., Braunwald, E., Jensen, M. D., Pories, W., Fahrbach, K. and Schoelles, K. (2004). Bariatric surgery: a systematic review and meta-analysis. *JAMA* **292**, 1724-1737.

Cummings, B. P., Digitale, E. K., Stanhope, K. L., Graham, J. L., Baskin, D. G., Reed, B. J., Sweet, I. R., Griffen, S. C. and Havel, P. J. (2008). Development and characterization of a novel rat model of type 2 diabetes mellitus: the UC Davis type 2 diabetes mellitus UCD-T2DM rat. *Am. J. Physiol. Regul. Integr. Comp. Physiol.* **295**, R1782-R1793.

Cummings, B. P., Stanhope, K. L., Graham, J. L., Baskin, D. G., Griffen, S. C., Nilsson, C., Sams, A., Knudsen, L. B., Raun, K. and Havel, P. J. (2010a). Chronic administration of the glucagon-like peptide-1 analog, liraglutide, delays the onset of diabetes and lowers triglycerides in UCD-T2DM rats. *Diabetes* **59**, 2653-2661.

Cummings, B. P., Stanhope, K. L., Graham, J. L., Evans, J. L., Baskin, D. G., Griffen, S. C. and Havel, P. J. (2010b). Dietary fructose accelerates the development of diabetes in UCD-T2DM rats: amelioration by the antioxidant, alpha-lipoic acid. *Am. J. Physiol. Regul. Integr. Comp. Physiol.* **298**, R1343-R1350.

Cummings, B. P., Strader, A. D., Stanhope, K. L., Graham, J. L., Lee, J., Raybould, H. E., Baskin, D. G. and Havel, P. J. (2010c). Ileal interposition surgery improves glucose and lipid metabolism and delays diabetes onset in the UCD-T2DM rat. *Gastroenterology* **138**, 2437-2446.

Cummings, B. P., Bettaieb, A., Graham, J. L., Stanhope, K. L., Kowala, M., Haj, F. G., Chouinard, M. L. and Havel, P. J. (2012). Vertical sleeve gastrectomy improves glucose and lipid metabolism and delays diabetes onset in UCD-T2DM rats. *Endocrinology* **153**, 3620-3632.

Folch, J., Lees, M. and Sloane Stanley, G. H. (1957). A simple method for the isolation and purification of total lipides from animal tissues. *J. Biol. Chem.* **226**, 497-509.

Furet, J. P., Kong, L. C., Tap, J., Poitou, C., Basdevant, A., Bouillot, J. L., Mariat, D., Corthier, G., Doré, J., Henegar, C. et al. (2010). Differential adaptation of human gut microbiota to bariatric surgery-induced weight loss: links with metabolic and low-grade inflammation markers. *Diabetes* **59**, 3049-3057.

Gregor, M. F., Yang, L., Fabbrini, E., Mohammed, B. S., Eagon, J. C., Hotamisligil, G. S. and Klein, S. (2009). Endoplasmic reticulum stress is reduced in tissues of obese subjects after weight loss. *Diabetes* **58**, 693-700.

Harding, H. P. and Ron, D. (2002). Endoplasmic reticulum stress and the development of diabetes: a review. *Diabetes* **51**, S455-S461.

Hotamisligil, G. S. (2010). Endoplasmic reticulum stress and the inflammatory basis of metabolic disease. *Cell* **140**, 900-917.

Kalaany, N. Y. and Mangelsdorf, D. J. (2006). LXRS and FXR: the yin and yang of cholesterol and fat metabolism. *Annu. Rev. Physiol.* **68**, 159-191.

Kohli, R., Kirby, M., Setchell, K. D., Jha, P., Klustaitis, K., Woollett, L. A., Pfluger, P. T., Balistreri, W. F., Tso, P., Jandacek, R. J. et al. (2010). Intestinal adaptation after ileal interposition surgery increases bile acid recycling and protects against obesity-related comorbidities. *Am. J. Physiol. Gastrointest. Liver Physiol.* **299**, G652-G660.

Li, J. V., Ashrafian, H., Bueter, M., Kinross, J., Sands, C., le Roux, C. W., Bloom, S. R., Darzi, A., Athanasiou, T., Marchesi, J. R. et al. (2011). Metabolic surgery profoundly influences gut microbial-host metabolic cross-talk. *Gut* **60**, 1214-1223.

Miyata, M., Yamakawa, H., Hamatsu, M., Kuribayashi, H., Takamatsu, Y. and Yamazoe, Y. (2011). Enterobacteria modulate intestinal bile acid transport and homeostasis through apical sodium-dependent bile acid transporter (SLC10A2) expression. *J. Pharmacol. Exp. Ther.* **336**, 188-196.

Morino, K., Petersen, K. F. and Shulman, G. I. (2006). Molecular mechanisms of insulin resistance in humans and their potential links with mitochondrial dysfunction. *Diabetes* **55 Suppl. 2**, S9-S15.

Nakatani, H., Kasama, K., Oshiro, T., Watanabe, M., Hirose, H. and Itoh, H. (2009). Serum bile acid along with plasma incretins and serum high-molecular weight adiponectin levels are increased after bariatric surgery. *Metabolism* **58**, 1400-1407.

Ozcan, U., Cao, Q., Yilmaz, E., Lee, A. H., Iwakoshi, N. N., Ozdelen, E., Tuncman, G., Görgün, C., Glimcher, L. H. and Hotamisligil, G. S. (2004). Endoplasmic reticulum stress links obesity, insulin action, and type 2 diabetes. *Science* **306**, 457-461.

Ozcan, U., Yilmaz, E., Ozcan, L., Furuhashi, M., Vaillancourt, E., Smith, R. O., Görgün, C. Z. and Hotamisligil, G. S. (2006). Chemical chaperones reduce ER stress and restore glucose homeostasis in a mouse model of type 2 diabetes. *Science* **313**, 1137-1140.

Patti, M. E., Houten, S. M., Bianco, A. C., Bernier, R., Larsen, P. R., Holst, J. J., Badman, M. K., Maratos-Flier, E., Mun, E. C., Pihlajamaki, J. et al. (2009). Serum bile acids are higher in humans with prior gastric bypass: potential contribution to improved glucose and lipid metabolism. *Obesity* **17**, 1671-1677.

Paulsen, S. J., Vrang, N., Larsen, L. K., Larsen, P. J. and Jelsing, J. (2010). Stereological assessment of pancreatic beta-cell mass development in male Zucker Diabetic Fatty (ZDF) rats: correlation with pancreatic beta-cell function. *J. Anat.* **217**, 624-630.

Pols, T. W., Noriega, L. G., Nomura, M., Auwerx, J. and Schoonjans, K. (2011). The bile acid membrane receptor TGR5 as an emerging target in metabolism and inflammation. *J. Hepatol.* **54**, 1263-1272.

Ron, D. and Walter, P. (2007). Signal integration in the endoplasmic reticulum unfolded protein response. *Nat. Rev. Mol. Cell Biol.* **8**, 519-529.

Samuel, V. T., Petersen, K. F. and Shulman, G. I. (2010). Lipid-induced insulin resistance: unravelling the mechanism. *Lancet* **375**, 2267-2277.

Sancho, V., Trigo, M. V., Martín-Duce, A., Gonz Lez, N., Acitores, A., Arnés, L., Valverde, I., Malaisse, W. J. and Villanueva-Peñacarrillo, M. L. (2006). Effect of GLP-1 on D-glucose transport, lipolysis and lipogenesis in adipocytes of obese subjects. *Int. J. Mol. Med.* **17**, 1133-1137.

Schauer, P. R., Kashyap, S. R., Wolski, K., Brethauer, S. A., Kirwan, J. P., Pothier, C. E., Thomas, S., Abood, B., Nissen, S. E. and Bhatt, D. L. (2012). Bariatric surgery versus intensive medical therapy in obese patients with diabetes. *N. Engl. J. Med.* **366**, 1567-1576.

Scott, W. R. and Batterham, R. L. (2011). Roux-en-Y gastric bypass and laparoscopic sleeve gastrectomy: understanding weight loss and improvements in type 2 diabetes after bariatric surgery. *Am. J. Physiol. Regul. Integr. Comp. Physiol.* **301**, R15-R27.

Shawl, A. I., Park, K. H. and Kim, U. H. (2009). Insulin receptor signaling for the proliferation of pancreatic β-cells: involvement of Ca2+ second messengers, IP3, NAADP and cADPR. *Islets* **1**, 216-223.

Sjöström, L., Lindroos, A. K., Peltonen, M., Torgerson, J., Bouchard, C., Carlsson, B., Dahlgren, S., Larsson, B., Narbro, K., Sjöström, C. D. et al. (2004). Lifestyle, diabetes, and cardiovascular risk factors 10 years after bariatric surgery. *N. Engl. J. Med.* **351**, 2683-2693.

Strader, A. D. (2006). Ileal transposition provides insight into the effectiveness of gastric bypass surgery. *Physiol. Behav.* **88**, 277-282.

Swann, J. R., Want, E. J., Geier, F. M., Spagou, K., Wilson, I. D., Sidaway, J. E., Nicholson, J. K. and Holmes, E. (2011). Systemic gut microbial modulation of bile acid metabolism in host tissue compartments. *Proc. Natl. Acad. Sci. USA* **108 Suppl. 1**, 4523-4530.

Thaler, J. P. and Cummings, D. E. (2009). Minireview: Hormonal and metabolic mechanisms of diabetes remission after gastrointestinal surgery. *Endocrinology* **150**, 2518-2525.

Thomas, C., Pellicciari, R., Pruzanski, M., Auwerx, J. and Schoonjans, K. (2008). Targeting bile-acid signalling for metabolic diseases. *Nat. Rev. Drug Discov.* **7**, 678-693.

Thomas, C., Gioiello, A., Noriega, L., Strehle, A., Oury, J., Rizzo, G., Macchiarulo, A., Yamamoto, H., Mataki, C., Pruzanski, M. et al. (2009). TGR5-mediated bile acid sensing controls glucose homeostasis. *Cell Metab.* **10**, 167-177.

Torchia, E. C., Labonté, E. D. and Agellon, L. B. (2001). Separation and quantitation of bile acids using an isocratic solvent system for high performance liquid chromatography coupled to an evaporative light scattering detector. *Anal. Biochem.* **298**, 293-298.

Watanabe, M., Houten, S. M., Mataki, C., Christoffolete, M. A., Kim, B. W., Sato, H., Messaddeq, N., Harney, J. W., Ezaki, O., Kodama, T. et al. (2006). Bile acids induce energy expenditure by promoting intracellular thyroid hormone activation. *Nature* **439**, 484-489.

Zhang, H., DiBaise, J. K., Zuccolo, A., Kudrna, D., Braidotti, M., Yu, Y., Parameswaran, P., Crowell, M. D., Wing, R., Rittmann, B. E. et al. (2009). Human gut microbiota in obesity and after gastric bypass. *Proc. Natl. Acad. Sci. USA* **106**, 2365-2370.